

Three-dimensional effects in *trans*-polyacetylene

S. Stafström

Department of Physics and Measurement Technology, University of Linköping, Linköping, Sweden

(Received 5 February 1985)

In a three-dimensional crystal of *trans*-polyacetylene we have considered different interchain orientations. Using a semiempirical self-consistent-field calculation scheme (modified neglect of differential overlap) we have calculated optimal values of the setting angle and total energies for different structures. The $(\text{CH})_x$ chains are found to be in phase along the horizontal and vertical crystal axes. In the glide plane, however, we found a degeneracy between the in-phase and out-of-phase orientations. The intrachain geometry is not affected by the surrounding chains as long as there are no solitons present on the chain. A segment between a soliton-antisoliton pair or between a soliton and a chain end, however, is confined due to interchain interactions. The confinement energy, here called the soliton-lattice energy, is 0.1 meV/(CH unit) in the soliton-bearing chain for a system initially in the ground-state configuration, leading to a confinement length at room temperature of about 250 CH units.

I. INTRODUCTION

Scanning electron micrographic studies¹ of films of polyacetylene show that the polymer chains build up fibrils with a diameter varying from 100 to 500 Å. These fibrils are randomly oriented. If one aligns the fibrils by stretching the polymer film, x-ray studies² show that the polymer chains are parallel to the fibril axis. From x-ray diffraction and electron-diffraction experiments it is also possible to determine the relative orientation of the polymer chains. Here, we restrict ourselves to the *trans* isomer, which is suggested to have the structure given in Fig. 1.^{2,3,4} Numerical values of the lattice parameters obtained by different groups and by different techniques are listed in Table I. Comparison with structural data from *trans*-diphenylpolyenes $\text{C}_6\text{H}_5(\text{C}=\text{C})_n\text{C}_6\text{H}_5$ suggests that *trans*-(CH)_x has a monoclinic symmetry and based on this the space group is either $P2_1/a$ or $P2_1/n$ depending on whether the single-bond—double-bond pattern on the two chains in the unit cell is either in phase or out of phase. Results quite different from those shown in Table I have been obtained from electron-diffraction experiments by Lieser *et al.*⁵ Here the different methods of polymerization, which use, for example, the Ziegler-Natta catalyst⁶

or the Luttinger catalyst,⁷ play an important role for the structure. The isomerization procedure is also important; it has been suggested⁸ that the $P2_1/n$ structure is the ground-state phase in polyacetylene while the $P2_1/a$ structure is obtained as a metastable intermediate state during the isomerization from all *cis*-(CH)_x to all *trans*-(CH)_x.

The degree of dimerization of *trans*-(CH)_x has also been experimentally determined. X-ray diffraction² shows that the carbon-atom distortion (see Fig. 1) is $u_0=0.026$ Å, resulting in single- and double-bond lengths of 1.44 Å and 1.36 Å, respectively. On the other hand, electron-diffraction experiments⁹ give $u_0=0.024$ Å and single- and double-bond lengths of 1.43 Å and 1.38 Å, respectively.

Most previous theoretical work on polyacetylene has been based on the Hückel theory including σ -bond compressibility. Within this model, the Su-Schrieffer-Heeger (SSH) model,¹⁰ it is possible to calculate self-consistently the dimerization pattern on a single chain¹¹ and fit it to experimental findings by adjusting the parameters included in the model. The Hubbard term, which contains the on-site electron-electron interaction, has been added to the SSH Hamiltonian. Monte-Carlo-type calcu-

TABLE I. Comparison of the unit-cell structure of *trans*-(CH)_x.

| | IP | IPR | IPR | OPR | OP | OP | x-ray fiber diffraction ^a | Electron diffraction ^b | BM calc ^c | BM calc ^c |
|----------|----------|----------|----------|----------|----------|----------|---|--------------------------------------|-------------------------|-------------------------|
| <i>a</i> | 4.24 | 4.24 | 4.24 | 4.24 | 4.24 | 4.24 | 4.24 | 7.32 | 4.25 | 4.25 |
| <i>b</i> | 7.32 | 7.32 | 7.32 | 7.32 | 7.32 | 7.32 | 7.32 | 4.24 | 7.32 | 7.32 |
| <i>c</i> | 2.50 | 2.50 | 2.50 | 2.50 | 2.50 | 2.50 | 2.46 | | 2.48 | 2.48 |
| β | 91.5 | 91.5 | 95.0 | 91.5 | 91.5 | 95.0 | 91.5 | | 90.5 | 91.1 |
| ϕ | 52.9 | 51.8 | 51.1 | 51.7 | 53.0 | 52.3 | 55.0 | 66 | 51.8 | 54.1 |
| | $P2_1/a$ | $P2_1/a$ | $P2_1/a$ | $P2_1/n$ | $P2_1/n$ | $P2_1/n$ | $P2_1/n$ | $Pnam$ | $P2_1/n$ | $P2_1/a$ |

^aReference 2.

^bReference 4.

^cReference 15.

lations¹² on small systems using this model show an enhancement of the dimerization for small values of the Hubbard U . Equilibrium structure of both the *cis* and *trans* isomer of polyacetylene has been determined from *ab initio* calculations by Karpfen and Petkov¹³ using a double- ζ technique. Semiempirical self-consistent-field calculations using the modified neglect of differential overlap (MNDO) scheme¹⁴ have also been applied to calculations of the ground-state geometry of a polyacetylene chain. Comparisons with experimental and *ab initio* studies show that geometry predictions are very accurate in the MNDO scheme and the three-dimensional-structure calculations in this paper will therefore be performed using this method.

Calculations concerning the geometry of the three-dimensional unit cell of polyacetylene have been done by Baughman *et al.*³ They minimize the lattice energy, which is the summation of the Williams 4 intermolecular potentials CC, CH, and HH. The unit-cell parameters are calculated for *trans*-(CH)_x using crystallographic data from diphenylpolyenes and assuming a monoclinic structure with $P2_1/a$ symmetry. In a later article by Baughman and Moss¹⁵ (BM), three different methods of calculating the lattice energy are presented. One method uses the Williams 4 potential; the second method uses the bond-bond interaction theory of Salem for the C-C dispersion and the Williams 4 potential for the C-C repulsion and the C-H and H-H repulsion and dispersion. In the third method, dynamic polarizability calculations of bond-bond dispersion between the C—C bond replaces the Salem method. Lattice-energy contributions are calculated using the three different methods and the results show a rather good agreement between the methods. The lattice energies of the $P2_1/a$ and $P2_1/n$ structures are calculated, giving a slightly lower energy for the $P2_1/n$ structure. BM also introduce the soliton-lattice energy E_{SL} , which is the change in energy due to a phase shift of π in the bond alternation of one chain surrounded by a lattice having its ground-state equilibrium geometry. Using the second and third methods they found that $E_{SL}=4$ cal/mol C₂H₂ [0.09 meV/(CH unit)] for the $P2_1/n$ symmetry and $E_{SL}=14$ cal/mol C₂H₂ [0.32 meV/(CH unit)] for the $P2_1/a$ symmetry. They also found that the six-nearest-neighbor chains contribute about 96% of the total value of E_{SL} . This result is used in this report where we have restricted the polyacetylene system to seven chains (see Fig. 1).

The problem of soliton confinement in polyacetylene due to interchain coupling is also treated by Baeriswyl and Maki¹⁶ who use the SSH Hamiltonian including an interchain hopping term t_1 on a system of two chains. Using values for the interchain and intrachain hopping energies $t_1 \approx 25$ –120 meV and $t_0 = 2.5$ eV, they found that an antiferromagnetic (out-of-phase) ordering between two chains is the ground-state configuration and the calculated soliton-lattice energy in a five-chain system is equal to $E_{SL} \approx 3$ –10 K per site. This method predicts out-of-phase ordering between all chains independent of their orientations. Other authors, such as, Baughmann and Moss always keep the in-phase orientation in the horizontal and vertical planes (see Fig. 1), which results in a unit

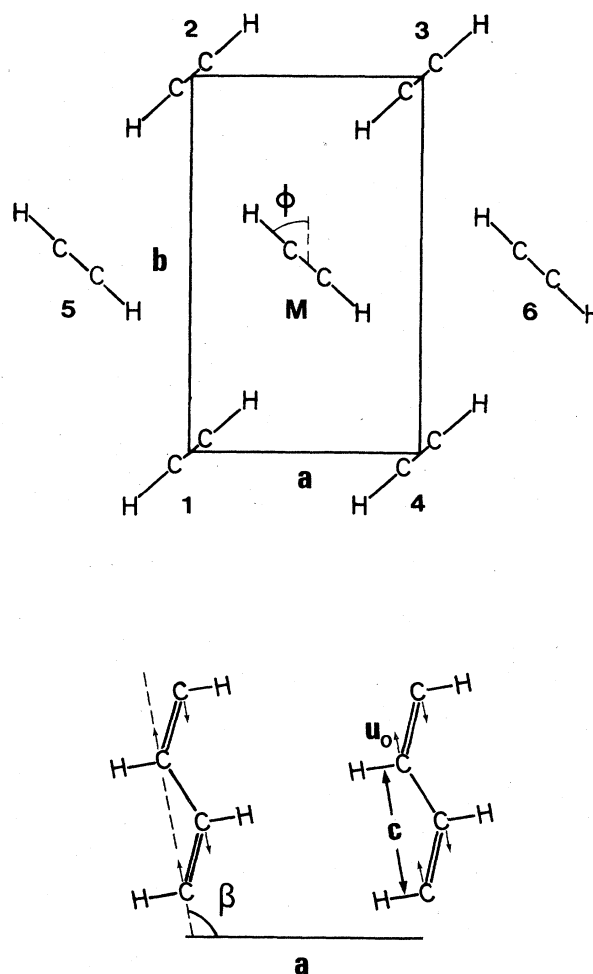


FIG. 1. Seven-chain *trans*-(CH)_x system viewed in the chain-axis direction (above) and with chains 1 and 4 projected on to the horizontal plane (below). ϕ is the setting angle and β is the monoclinic angle.

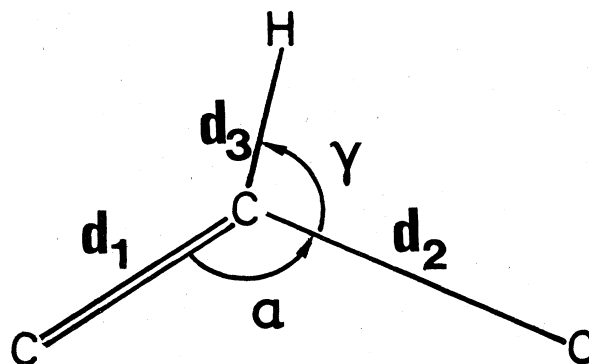


FIG. 2. Intrachain geometry of *trans*-(CH)_x. Our calculated values are $d_1 = 1.3584$ Å, $d_2 = 1.4642$ Å, $d_3 = 1.09$ Å, $\alpha = 124.95^\circ$, and $\gamma = 115.6^\circ$.

cell of three-dimensional (3D) $(\text{CH})_x$ built up from two chains in the same glide plane (chain 1 and the middle chain in Fig. 1). In this article we will compare total energies of the in-phase and out-of-phase orientations of chains in the horizontal plane and in the glide plane. We will also determine the relaxed intra-chain and interchain geometry of the system shown in Figs. 1 and 2 and finally calculate the soliton-lattice energy for the system.

II. METHOD OF CALCULATION

As mentioned in Sec. I, Boudreaux *et al.*¹⁴ have shown that the MNDO scheme of Dewar and Theil¹⁷ gives a very good prediction of the chain geometry for polyacetylene. It is therefore reasonable to assume that the three-dimensional-structure calculated by this method is also of good quality. MNDO is a semiempirical method for finding the self-consistent-field solutions of the Roothaan equations with a basis set consisting of the valence atomic orbitals of the calculated molecule. Certain selected sets of multicenter integrals are neglected and other terms in the equations are determined either from experimental data or from semiempirical expressions which contain numerical parameters that are adjusted to optimize molecular geometries and heats of formation ΔH_f :

$$\Delta H_f = E_{\text{tot}} - E_{\text{el}} + \sum_A \Delta H_f^A$$

and

$$E_{\text{tot}} = E_{\text{el}} + \sum_A \sum_{\substack{B \\ (A < B)}} E_{AB}^{\text{core}}$$

The summations are over all atoms in the molecule. E_{AB}^{core} are the core-core repulsions, E_{tot} is the total energy of the molecule, and E_{el} is the total electronic energy of the molecule.

Since the aim of this report is to calculate geometrical data for different structures of the three-dimensional unit cell of polyacetylene and to compare total energies of these structures, the MNDO scheme is ideal for our purpose. Other data, such as, the band gap and the energies of individual molecular-orbital (MO) states that are less accurate in MNDO are not presented here. Another great advantage of MNDO compared to *ab initio* methods is that the approximations made in the MNDO scheme make computations of relatively large systems possible. Since in our calculation we need up to seven chains (see Fig. 1), it is still a very time-consuming project.

The interchain distances a and b cannot be optimized in the seven-chain system and will therefore be held fixed. Numerical values of a and b are taken from x-ray-diffraction studies by Fincher *et al.*²: $a = 4.24$ Å and $b = 7.32$ Å. Also, the monoclinic angle β will be fixed but two different values, $\beta = 91.5^\circ$ and $\beta = 95.0^\circ$, are used in two otherwise identical sets of computations. The setting angle ϕ will be optimized separately in the $P2_1/a$ and $P2_1/n$ symmetries. The optimization is done iteratively by guessing one starting value ϕ_0 for the six surrounding chains and letting ϕ on the middle chain vary to lower the total energy. The optimized value ϕ_1 is the input setting angle of the six surrounding chains in the second itera-

tion. This procedure is then repeated until self-consistency in ϕ is obtained. Using the optimized value of the setting angle we optimize the chain geometry in the same iterative way by fixing the geometry of the surrounding chains and letting all the bond lengths and bond angles on the middle chain vary to lower the energy. In this case, however, there is in principle no need to iterate since it is found that the intrachain geometry is not affected by the surrounding chains as long as no solitons or polarons are present. Once the optimized geometry is found we can calculate differences in heat of formation and total energy between different structural configurations.

III. RESULTS AND DISCUSSION

With the fixed values on the geometrical parameters a , b , and β , we have optimized the setting angle in the seven-chain system. Each of chains 1 to 6 (see Fig. 1) contain six double bonds, i.e., $\text{C}_{12}\text{H}_{14}$, and the termination unit is $=\text{CH}_2$. It is worthwhile to stress that *trans*- $(\text{CH})_x$ chains always end with double bonds. The intrachain geometry is taken from the optimized values of a single-chain system. These values are, for the double bond ($\text{C}=\text{C}$), $d_1 = 1.3583$ Å, the single bond ($\text{C}-\text{C}$), $d_2 = 1.4640$ Å, the $\text{C}-\text{H}$ bond, $d_3 = 1.09$ Å, the $\text{C}-\text{C}=\text{C}$ angle, $\alpha = 124.9^\circ$, and the $\text{H}-\text{C}-\text{C}$ angle, $\gamma = 115.6^\circ$. Suppose that the unit cell of $(\text{CH})_x$ in three dimensions consists of a C_2H_2 unit from two chains in the same glide plane, say, chain 1 and the middle chain in Fig. 1. Note that under this assumption, the chains in the same horizontal plane are in phase. With fixed interchain distance we can think of four different orientations that can give local minima in the total energy. These orientations are shown in Fig. 3 viewed in the chain-axis direction and projected on the horizontal plane. The different orientations in parts (a), (b), (c), and (d) are as follows: (a) in phase (IP), (b) in phase and rotated by π (IPR), (c) out of phase and rotated by π (OPR), (d) out of phase (OP). To be able to do comparable calculations on different symmetries and to calculate the soliton-lattice energy, it is necessary to be able to shift and rotate the middle chain without changing the energy due to interactions involving

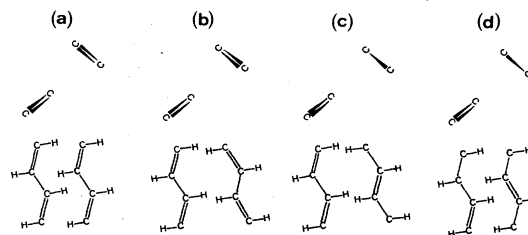


FIG. 3. Different possible interchain orientations of the unit-cell chains, chain 1 and the middle chain. (a) The chains are in phase; (b) the chains are in phase but the middle chain is rotated by π about the chain axis direction; (c) the chains are out of phase but the middle chain is rotated by π ; (d) the chains are out of phase.

the chain ends. To avoid this effect we let the middle chain be longer than the surrounding chains, here, the middle chain contains ten double bonds, i.e., $C_{20}H_{22}$, which means that the ends of this chain will always be far away from the ends of the surrounding chains. With this geometry the setting angle is optimized following the iterative procedure described in Sec. II. The results converge after about five iterations with an accuracy of roughly 0.02° in the final value of ϕ . Table I, columns 1–6 provide the optimized values of the setting angle for two different monoclinic angles β and for the different orientations described above. Columns 7–9 provide results, both theoretical and experimental, from works of other authors.

During the optimization procedure we found that the setting angle of the middle chain results from competition between chains 1–4, on the one hand, and chains 5 and 6, on the other hand. Mainly, the electron-electron repulsion energy between orbitals attached to close-lying hydrogen and carbon atoms connected to different chains is minimized to determine the optimal value of ϕ in the ground state of the seven-chain system. A five-chain system containing chains 1–4 and the middle chain will relax to the optimal setting angle 90° . If only the chains in the horizontal plane are treated, the resulting value of ϕ is 0° . The smaller value of the setting angle in the rotated structure can also be explained in terms of electron-electron repulsion between electrons occupying the molecular orbital localized mainly on a hydrogen atom and a π electron which sticks out normal to the plane of the polyacetylene chain and points in the direction of the hydrogen atom. If we look at Fig. 1 we can recognize the rotated structure as the one in which all the carbon atoms in the plane normal to the chain axis are in the same intrachain position, while in the unrotated structure, the carbon-atom positions are changed on the chains in the horizontal plane containing the middle chain. A careful study of the overlap between the π -electron MO's on the middle chain and the MO's localized on the close-lying hydrogen atoms in chains 1–4, shows that this overlap is smaller in the rotated structure. As mentioned earlier, the value of ϕ on the middle chain results from a competition between chains 1–4, on the one hand, and chains 5 and 6, on the other hand. Since the interaction between the middle chain and chains 5 and 6 is unchanged, and that between chains 1–4 is weakened in the rotated structure, the setting angle is then reduced.

As can be seen from Table I, we found a very small difference in the setting angle between the in-phase and out-of-phase structures. This is reasonable since the displacement of the carbon atoms is very small ($u_0 = 0.03$ Å) compared to the interchain distances. Similarly, the two different values of the monoclinic angle do not give any large change in the setting angle, which is also expected since a change in β does not change the distance between nearest neighbors on neighboring chains. Only more distant neighbors on different chains in the same horizontal plane come closer when β is increased.

A comparison (see Table I) shows that our values of ϕ are rather close to both the experimental value of Fincher *et al.*² and what has been calculated by Baughmann and Moss. In their works the interchain orientation is denoted

by the space-group assignments $P2_1/a$ and $P2_1/n$ representing the in-phase and out-of-phase orientations, respectively. However, these assignments do not specify whether or not one chain in the unit cell is rotated by π about its axis. From Fig. 2 in Ref. 15 one can see that they treat only the cases denoted by IP ($P2_1/a$) and OPR ($P2_1/n$) in this report. Their calculated values of ϕ and β shown in Table I come from these two orientations and agree very well with what we found from the MNDO calculations. Our findings that the optimal value of ϕ is smaller in the rotated orientation than that in the unrotated one and that ϕ gets smaller when β is increased, are also in agreement with what BM found.

To check the finite-size effect on the optimal value of the setting angle, we repeat the calculations with chains 1–6 reduced to C_6H_8 and the middle chain reduced to $C_{12}H_{14}$. In these smaller systems we found slightly larger values of the setting angle. The increase is, however, less than 1.0° in all cases. With such a small change in ϕ , we are convinced that the values given in Table I, columns 1–6 are rather close to what should be found in an infinite system.

Concerning the intrachain geometry, we found in a single-chain system the following values of the geometrical parameters (see Fig. 2): $d_1 = 1.463$ Å, $d_2 = 1.357$ Å, $d_3 = 1.09$ Å, $\alpha = 124.9^\circ$, and $\gamma = 115.7^\circ$. These values are adopted for all chains in the seven-chain system and kept fixed during the setting-angle optimization. Once the value of ϕ is found, we look for the optimized values of the intrachain lattice constants in the seven-chain system, with only the restriction that the backbone structure be planar. The new values are $d_1 = 1.464$ Å, $d_2 = 1.358$ Å, $d_3 = 1.09$ Å, $\alpha = 124.95^\circ$, and $\gamma = 115.5^\circ$. Surprisingly, the H–C–C angle γ is almost independent of the interchain orientation. We also found that the hydrogen atoms always lie in the same plane as the carbon atoms. The values of d_1, d_2 , and α result in a distance between two CH units of $c = 2.5036$ Å (see Fig. 1) and a CH unit displacement of $u_0 = 0.030$ Å. From these very small changes in the intrachain lattice constants we can conclude that the intrachain, ground-state geometry is not affected by the surrounding chains. However, as we shall see later, there is a change in total energy involved in a phase shift of π of one chain with respect to a neighboring chain, which will affect the intrachain structure if topological excitations, such as, soliton-antisoliton pairs are present on the chain. We will come back to this interesting question later in this section.

Knowing the different geometries we can calculate and compare their respective total energies. A difficulty when calculating total energies for systems containing up to seven chains, is that the surface is very large compared to the bulk. We believe that this causes no problem as long as we only qualitatively compare energies of different interchain orientations in otherwise identical systems. A quantitative comparison between our results and other works is more uncertain. Numerical values of energies presented below will be normalized either with the total number of CH units in the system, or with the number of CH units in one chain. The latter way of normalizing is used when we calculate the soliton-lattice energy, which

TABLE II. Heat of formation ΔH_f , total energy E_{tot} , electronic energy E_{el} , core repulsion energy E_{AB}^{core} for the seven-chain system [in eV/(CH unit)], and soliton-lattice energy E_{SL} [in meV/(CH unit of the soliton bearing chain)].

| | IP | IPR | OPR | OP |
|------------------------|-----------|-----------|-----------|-----------|
| ΔH_f | 0.3497 | 0.3484 | 0.3484 | 0.3496 |
| E_{tot} | -144.3365 | -144.3378 | -144.3378 | -144.3366 |
| E_{el} | -2427.503 | -2427.417 | -2424.902 | -2425.714 |
| E_{AB}^{core} | 2283.167 | 2283.079 | 2280.564 | 2281.377 |
| E_{SL} | | 0.1 | 0.1 | |

then will be independent of the size of the system.

The difference in total energy between the different alignments of chains in the same horizontal plane is calculated in a three-chain system containing the middle chain and chains 5 and 6 (see Fig. 1). We found that the in-phase alignment is the most stable configuration. This means that we have confirmed the previous assumption that the unit cell of *trans*-(CH)_x consists of two chains only. The difference in total energy between the in-phase and out-of-phase orientations is, however, small, only 0.5 meV/(CH unit). Two more orientations are possible if the middle chain is rotated by π around its axis. Given this rotation, we found a difference in total energy, with respect to the ground state, of 1.2 and 1.7 meV/(CH unit) for the out-of-phase and in-phase orientations, respectively. Next, we repeat the calculations in a five-chain system (containing the middle chain and chains 1–4). Here, we found two almost degenerate ground-state interchain orientations, namely, the OPR and IPR orientations [see Figs. 3(b) and 3(c)]. In fact, OPR has lower energy but difference is only 0.01 meV/(CH unit) which probably is less than the accuracy of the program. About 1.0 and 1.5 meV/(CH unit) higher up in the total energy we found the OP and IP orientations, respectively. Given the in-phase alignment in the horizontal plane, the ground state for the seven-chain system should then also exhibit a degeneracy in total energy between the OPR and IPR structures. Using the optimized value of the setting angle we have calculated the total energy for this system and compared it with the other possible orientations shown in Fig. 3. The numerical result, given in Table II, shows that there is a jump of about 1.2 meV/(CH unit) in total energy between the rotated and unrotated orientations. If, however, some external force, from, for example, the end groups, bending of the fiber, or other kinds of disorder, will force the chain into larger setting angles, the total energy of the rotated (OPR and IPR) orientations will exceed the total energy of the unrotated (OP and IP) orientations which then become the ground-state configuration. The increase in energy of the OPR orientation when the setting angle is increased from its optimal value (51.75°) to 55° is roughly 1 meV/(CH unit). This rather small energy difference shows that fluctuations in the value of ϕ are expected.

The x-ray-diffraction experiments of Fincher *et al.*,² who found $\phi=55^\circ$ and a $P2_1/n$ structure and the results obtained by BM agree with our findings. Given the monoclinic angle $\beta=91.4^\circ$, BM derive the setting angle ϕ by minimizing lattice energy. These values of ϕ are then

used to calculate the total lattice energy. The optimized setting angles they found were $\phi=51.8^\circ$ in $P2_1/n$ (OPR) and $\phi=54.0^\circ$ in $P2_1/a$ (IP), and the difference in total lattice energy is 0.06 kcal/(mol C₂H₂) [1.3 meV/(CH unit)] where the $P2_1/n$ structure has the lowest energy. From Table II we can see that our calculated difference in energy between the OPR and IP orientations also is 1.3 meV/(CH unit).

Chien⁸ has suggested that the OPR orientation (structure C, Fig. 3.24, p. 119 of Ref. 9) is the product of long-time thermal isomerization and that the IPR orientation (structure B) is a metastable structure obtained during the process of isomerization. Going from IPR to OPR involves a rotation by π around the chain axis of one chain in each unit cell. This motion has a very high energy barrier to pass and can only occur at high isomerization temperatures ($T \approx 400$ K), provided that at these temperatures, the OPR phase is a state of lower energy than the IPR phase. If the temperature is lowered before a homogeneous OPR phase is obtained, the sample will consist of a mixture of the two phases. Since the isomerization involves a lot of rotations it is very likely that the sample also will contain IP and OP phases, but these phases can more easily, through a shift of one chain, relax to OPR and IPR. In general, one can say that less carefully performed isomerization will result in *trans*-(CH)_x chains rotated in many different ways. Concerning the intrachain properties this rotation can reduce or even cut out the π -electron overlap. This shortening of the conjugation length has been experimentally verified from the dispersion of the Raman spectra taken on *trans*-polyacetylene.¹⁸

If a soliton-antisoliton pair ($S\bar{S}$) is introduced on the middle chain in the seven-chain system, the segment between the kinks will give rise to additional interchain in-

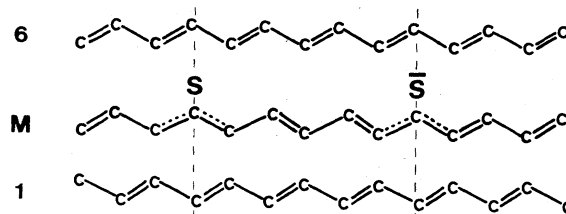


FIG. 4. Projection of the middle chain (*M*) and the chains 1 and 6 on the horizontal plane. The area between the dashed lines contains the region between the soliton (*S*) and antisoliton (\bar{S}).

teraction energy; following BM we will call this energy the soliton-lattice energy E_{SL} . Given the OPR (IPR) orientation, the segment on the middle chain between the kink and antikink will be out of phase with respect to chains 5 and 6 but in phase (out of phase) and rotated by π with respect to chains 1–4. Figure 4 shows how the interchain orientation is changed if the middle chain bears a $S\bar{S}$ pair. We know from the calculations above that the out-of-phase ordering in the horizontal plane is energetically unfavorable, while the two different orientations in the glide plane are degenerate. One would therefore expect a soliton-lattice energy, approximately equal to the increase in energy due to the out-of-phase ordering between chains 5 and 6 and the middle chain, which from the calculation in the three-chain system is 0.5 meV/(CH unit). However, due to the different polarization of the electron cloud in the seven-chain system, this chain difference is reduced. Our calculated value of the soliton-lattice energy is 0.1 meV/(CH unit) in the middle chain. This value holds for the system initially either in the OPR or in the IPR orientations. As mentioned in the introduction BM also calculated the soliton-lattice energy and found $E_{SL} = 4$ cal/mole C_2H_2 (or 0.09 meV/CH) in the soliton-bearing chain in the $P2_1/n$ (OPR) structure, which again is surprisingly close to the value calculated from the MNDO scheme.

The existence of highly mobile spins in *trans*-(CH) $_x$ is experimentally verified^{19–21} and is interpreted¹⁰ as neutral solitons which have a small activation barrier for translational motion. Low-temperature electron-nuclear double-

resonance (ENDOR) studies^{20,21} suggest a diffusion length of about 50 CH units.²² Narrowing of the ENDOR spectrum with increasing temperature shows that the mobility of the soliton increases due to the larger confinement length. For n CH units between a soliton and antisoliton, or between a soliton and a chain end, we have an increase in total energy of $E_n = nE_{SL}$, which at temperature T implies a soliton confinement length of $n_c = k_B T / E_{SL}$. At room temperature, $n_c \approx 250$ CH units. It is, however, unrealistic to think that this value also could be found from experiment since a real material always contains disorder. The disorder effect will produce local variations in the interaction energy, which easily can exceed, or cancel the small value of the soliton-lattice energy found in our calculations. Dopant molecules, such as, AsF_5 have been shown²³ to increase the thickness of the fibril containing the polyacetylene chains and therefore, to a great extent, change interchain distances and orientations. The motion of solitons created by doping will therefore be even more controlled by the disorder effects. Still, the three-dimensional interactions will be of importance and must be considered in future studies of soliton transport.

ACKNOWLEDGMENTS

I would like to thank Dr. K. A. Chao for many stimulating discussions. This work is financially supported by the Swedish Natural Science Research Council under Grants No. NFR-FFR-3996-113 and No. NFR-F-3996-124.

¹D. C. Bott, C. K. Chai, D. L. Gerrard, R. T. Weatherhead, D. White, and K. P. J. Williams, in *Proceedings of the International Conference on the Physics and Chemistry of Conducting Polymers, Les Ares, France*, edited by R. Comes [J. Phys. **44**, C3 (1983)].

²C. R. Fincher, Jr., C.-E. Chen, A. J. Heeger, and A. G. MacDiarmid, Phys. Rev. Lett. **48**, 100 (1982).

³R. H. Baughmann, S. L. Hsu, L. R. Anderson, G. P. Pez, and A. J. Signorelli, *Molecular Metals*, Vol. 1, Series VI of *NATO Conference Series*, edited by W. E. Hatfield (Plenum, New York, 1979), p. 187.

⁴K. Shimamura, F. E. Karasz, J. A. Hirsch, and J. C. W. Chien, Macromol. Chem. **2**, 473 (1981).

⁵G. Lieser, G. Wegner, W. Müller, and V. Enkelmann, Macromol. Chem. **1**, 621 (1980).

⁶T. Ito, H. Shirakawa, and S. Ikeda, J. Polym. Sci., Polym. Chem. Ed. **12**, 11 (1974).

⁷L. B. Luttinger, Chem. Ind. (London) **36**, 1133 (1960).

⁸J. C. W. Chien, *Polyacetylene* (Academic, London, 1984).

⁹J. C. W. Chien, Macromol. Chem. **3**, 655 (1982).

¹⁰W. P. Su, J. R. Schrieffer, and A. J. Heeger, Phys. Rev. Lett. **42**, 1698 (1979); Phys. Rev. B **22**, 2099 (1980).

¹¹S. Stafström and K. A. Chao, Phys. Rev. B **29**, 7010 (1984).

¹²J. E. Hirsch, Phys. Rev. Lett. **51**, 296 (1983).

¹³A. Karpfen and J. Petkov, Theor. Chim. Acta **53**, 65 (1979).

¹⁴D. S. Boudreaux, R. R. Chance, and J. L. Bredas, Phys. Rev. B **28**, 6927 (1983).

¹⁵R. H. Baughmann and G. Moss, J. Chem. Phys. **77**, 6321 (1982).

¹⁶D. Baeriswiel and K. Maki, Phys. Rev. B **28**, 2068 (1983).

¹⁷M. J. S. Dewar and W. Thiel, J. Am. Chem. Soc. **99**, 4889 (1977); **99**, 4907 (1977).

¹⁸F. B. Schügerl and H. Kuzmany, J. Chem. Phys. **74**, 953 (1981).

¹⁹B. R. Weinberger, E. Ehrenfreund, A. Pron, A. J. Heeger, and A. G. MacDiarmid, J. Chem. Phys. **72**, 4749 (1980).

²⁰S. Kuroda and H. Shirakawa, Solid State Commun. **43**, 591 (1982).

²¹H. Thomann, L. R. Dalton, Y. Tomkiewicz, N. S. Shiren, and T. C. Clarke, Phys. Rev. Lett. **50**, 533 (1983).

²²A. J. Heeger and J. R. Schrieffer, Solid State Commun. **48**, 207 (1983).

²³A. J. Epstein, H. Rommelmann, R. Fernquist, H. W. Gibson, M. A. Drury, and T. Woerner, Polymer **23**, 1211 (1982).